Received: 21 September 2022 | Revised: 27 January 2023 | Accepted: 28 January 2023

DOI: 10.1002/vnl.21984

RESEARCH ARTICLE

JOURNAL OF Vinyl & Additive TECHNOLOGY WILEY

Rheological characterization of linear low-density polyethylene–Fischer–Tropsch wax blends

Thobile Mhlabeni | **Cebo Ngobese** | **Shatish Ramjee** | **Walter Focke**

Department of Chemical Engineering, Institute of Applied Materials, University of Pretoria, Pretoria, South Africa

Correspondence
Shatish Ramjee, Department of Chemical Engineering, Institute of Applied Materials, University of Pretoria, Private Bag X20, Hatfield 0028, Pretoria, South Africa.
Email: shatish.ramjee@up.ac.za

Funding information
Sasol, Grant/Award Number: 126/20 GT

Abstract

The thermal and rheological behavior of blends of a Fischer–Tropsch (F-T) wax with linear low-density polyethylene (LLDPE) were investigated by differential scanning calorimetry and cone-and-plate rheometry. F-T wax is used as a possible low-cost processing aid alternative for LLDPE masterbatch applications. The melting- and crystallization thermograms indicated a two-phase solid-state morphology and full compatibility in the fully molten material. Both the high-melting and low-melting phase contained co-crystalized wax and polymer. Rheological data of F-T wax-LLDPE blends over the full composition range was also obtained. The zero-shear viscosity data was adequately predicted by the Friedman and Porter mixing rule: $\eta = \left(w_p \eta_p^{1/\alpha} + w_w \eta_w^{1/\alpha}\right)^{\alpha}$ with $\alpha = 3.4$. This implies that the melt viscosity is dominated by the effects of polymer chain entanglement and that the main consequence of adding the wax is to reduce the concentration of the polymer present. The complex viscosity also fitted this model albeit with $\alpha = 4.81$. All Han plots, that is, plots of the logarithm of the storage modulus (G') against the logarithm of the loss modulus (G''), were linear. Within the experimental uncertainty, they were essentially unaffected by variations in blend composition, temperature and the applied angular frequency. Additionally, Cole–Cole plots were also in agreement that wax-LLDPE blends are miscible at melt state. This supports full miscibility of the F-T wax-LLDPE blend system down to temperatures as low as 120°C.

KEYWORDS
compatibility, polyethylene, wax

1 | INTRODUCTION

Blends of waxes with polyethylene are of interest in numerous technical applications. They are of interest in the formulation of phase-change materials for thermal energy storage,[1–3] investment casting molding compounds,[4] materials for rapid prototyping by fused deposition modeling[5] and machinable waxes.[6] Waxes also find extensive application as processing additives in polymer compounding applications. For instance, polyethylene and polypropylene waxes are used to enhance melt flow and facilitate

better mixing of fillers and pigments in masterbatch compounding operations.[7] However, besides the already established technical processing aids, the plastics industry is continuously developing new polymeric materials including additives to deliver similar requirements at lower costs. For this purpose, the utilization of Fischer–Tropsch (F-T) wax as a possible alternative processing aid is explored. Processing additives based on waxes have some challenges regarding its compatibility with the base polymer matrix. Poor compatibility makes it difficult to process the polymer-additive mixture using conventional industrial processing techniques such as extrusion and injection molding.[7] F-T wax, because it is largely constituted of straight chain alkanes, is likely to show good blending characteristics with polymers in the polyethylene family.[1–3]

The thermal and mechanical properties of wax-polyethylene blends have been studied extensively.[1,8–11] In particular, Mpanza and Luyt[9] investigated F-T waxes as additives for increasing the melt flow index (MFI) of low-density polyethylene (LDPE). However, the rheological behavior, over the full range of compositions, has received limited attention.[12,13] The apparent viscosity behavior, at both low and at high shear rates, is of interest for the technical applications mentioned above. Apart from providing useful data on the effects of blend composition, temperature and shear rate on the apparent viscosity, such studies can also provide information on the compatibility of the two components in the molten-liquid state.[14–16] Therefore, this study considered the rheological characterization of blends of a F-T wax, specifically designed as a polyethylene processing agent, with a linear low-density polyethylene (LLDPE). The performance of this system, in highly filled calcium carbonate masterbatches, is reported elsewhere.[17,18]

2 | MATERIALS AND METHODS

2.1 | Materials

LLDPE grade HM2420 was supplied by Sasol. The density of this grade was 924 kg m^{-3} and the Melt Index was 20 g 10 min^{-1} @ 190°C 2.16 kg^{-1}. The number average molecular weight (M_n) and the weight average molecular weight (M_w) of the LLDPE were 23 530 and 129 100 Dalton, respectively. The polymer was milled into a powder (<400 μm) by Dream Weaver. Sasol also provided an experimental F-T wax in the form of pellets. The number average (M_n) and weight average (M_w) molar mass of this wax were 776 and 786 Dalton, respectively.

2.2 | Sample preparation

Wax-LLDPE blends were prepared by extrusion compounding on a ThermoFischer TSE 24 co-rotating twin-screw compounder (24 mm Φ, 30 L/D). The die had a single exit hole with a diameter of 5.5 mm. The screw speed was set at 50 rpm. The temperature profile was set as follows, 60/110/140/170/170/170/170°C. The blend containing 90 wt% wax was prepared differently as the low melt viscosity posed processing problems. The mixture was placed in aluminum pans and covered with aluminum foil and heated in an oven set at a temperature of 170°C. After 30 min, the fully molten liquid mixture was vigorously stirred, then left in the oven for an additional 30 min. This was done to ensure that near perfect homogenization of the materials via molecular diffusion has taken place.

2.3 | Sample characterization

2.3.1 | Differential scanning calorimetry

Thermal analysis was performed on a Perkin Elmer DSC 4000 analyzer. The samples (15 ± 1 mg) were crimped in 50 μL aluminum pans with pin-hole lids. An inert atmosphere was ensured by using nitrogen gas flowing at a rate of 20 mL min^{-1}. The thermal history of each sample was erased by holding it for 5 min at 170°C. For the non-isothermal crystallization study, the temperature was cycled between 30 and 170°C at a scan rate of 10°C min^{-1}. The second heating and cooling scans were used to determine the peak melting temperature (T_m) and peak crystallization temperature (T_c).

2.3.2 | Rheometry

The samples were subjected to rheological characterization on an Anton Paar MCR301 Rheometer fitted with a cone and plate configuration. Shear experiments were conducted isothermally at temperatures of 160, 170, and 180°C. After heating to the measurement temperature, the sample was squeezed down to a gap setting of 0.051 mm. The sample was pre-sheared for 1 min at a shear rate of 5 s^{-1} followed by 1 min of rest. The viscosity data were collected at applied shear rates varying from 0.01 to 100 s^{-1}. The complex viscosity, loss modulus, and storage modulus were determined using frequency sweeps in the oscillatory mode. The applied frequency was scanned from 100 to 1 rad s^{-1} at selected isothermal temperature and fixed strain of 0.05%. The

complex viscosity was also determined using temperature sweeps in the oscillatory mode. In these experiments, the temperature was scanned from 180 to 120°C at a fixed strain of 0.05% and an angular frequency of 10 rad s^{-1}

3 | RESULTS AND DISCUSSIONS

3.1 | Differential scanning calorimetry wax-LLDPE melting and crystallization behavior

Figure 1 presents typical differential scanning calorimetry (DSC) melting and crystallization curves obtained for the wax-LLDPE blends. The curves are plots of the normalized heat flux versus temperature with the orientation of the curves such that endothermic processes appeared up and exothermic processes appeared down. These results represent the melting and crystallization processes of the blends obtained from the second and third scans for the purpose of comparisons. In the pure state, the wax displays a broad melting curve with a doublet peak while the LLDPE featured a single, narrower melting peak. Due to the broad nature and the poor resolution between the two peaks due to the wax, it was rather difficult to analyze the melting peaks with increasing LLDPE concentration. However, it is clear that the original two wax peaks tend to merge into one single wax peak as the LLDPE content of the blend is increased.

In order to assess the extent of compatibility, the melting and crystallization curves are reproduced in Figure 2. The experimental DSC results are compared to the predictions based on mass fraction-weighted combinations of the DSC traces obtained for the neat wax and LLDPE. Figure 2A shows the results for the blend containing 10 wt% LLDPE. The melting peak, at the highest temperature, is associated with the LLDPE-rich phase. It is noteworthy that this peak has shifted to a significantly lower temperature and that its intensity has increased. The latter observation indicates that portion of the wax must have co-crystallized with the LLDPE. Furthermore, this means that this part of the wax now has a higher melting point than what it had when present in the neat wax. This portion probably derived from that part of the wax responsible for the second wax melting peak. This is indicated by the fact that the heat flux in in this region was disproportionally reduced when compared to that of the lower melting peak of the wax.

In Figure 2B the difference between the melting curves, measured and calculated for the blend containing 30 wt% LLDPE, is particularly striking. The peak attributed to the LLDPE-rich phase has shifted to even lower temperatures but now the intensity is about the same as would be expected for the neat polymer. However, the heat flux in the wax-rich regions has increased significantly. This suggests that a portion of the LLDPE, which would normally remain amorphous, co-crystalized with the wax. This increase in the specific enthalpy is also reflected in the crystallization exotherms.

Figure 2C,D show the results obtained at higher LLDPE content. The changes in both of the two melting endotherms and the two crystallization exotherms curves are striking. They are consistent with the notion of co-crystallization having happened in both the wax-rich phase and the LLDPE-rich phases. Figure 3 plots

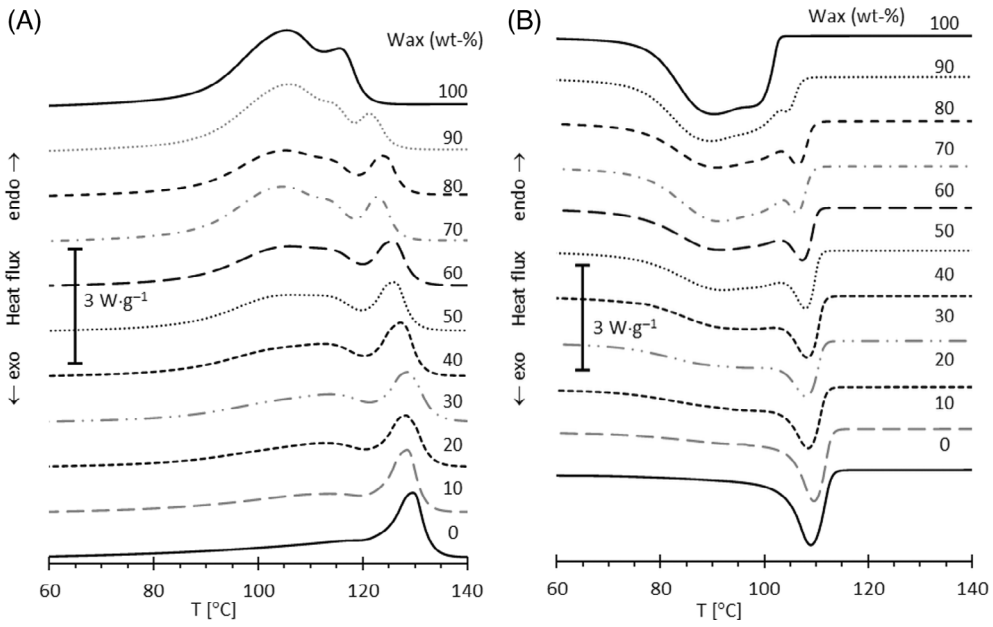

FIGURE 1 Typical differential scanning calorimetry (DSC) curves for the wax-linear low-density polyethylene (LLDPE) blends. (A) Melting during heating scans and (B) crystallization during cooling scans.

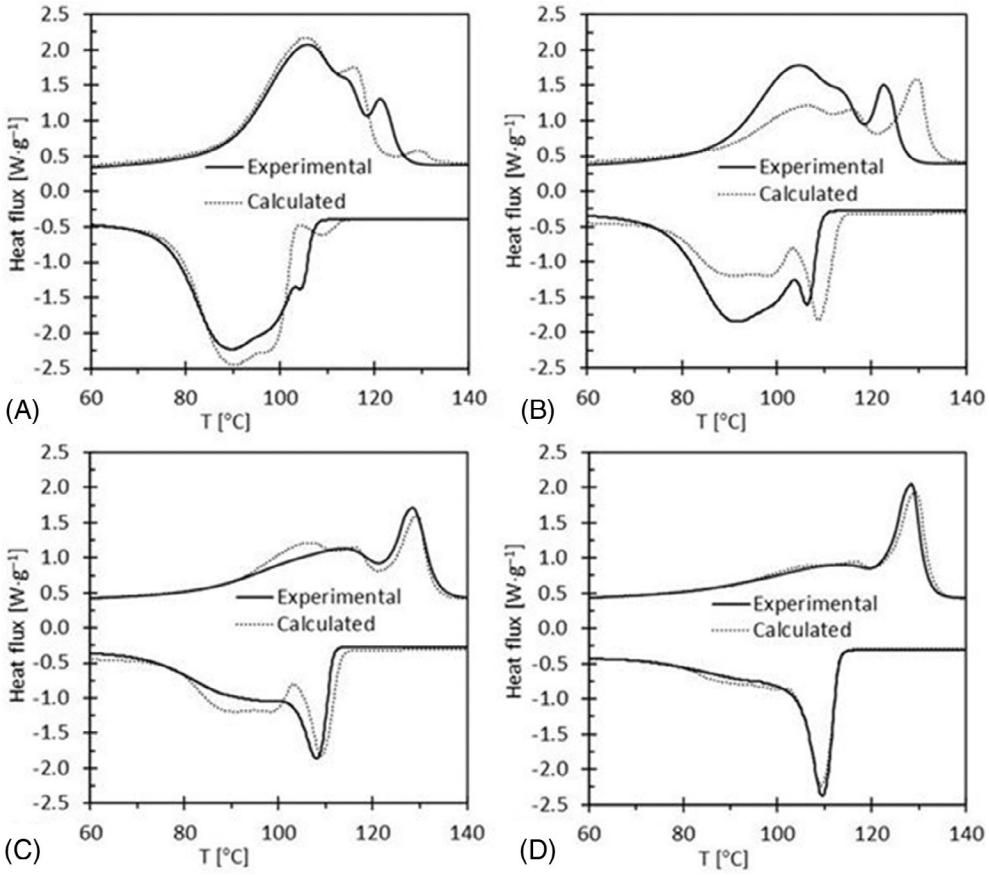

FIGURE 2 Comparing measured and predicted melting and crystallization curves for (A) 90–10, (B) 70–30, (C) 30–70, and 10–90 wax-linear low-density polyethylene (LLDPE) blends.

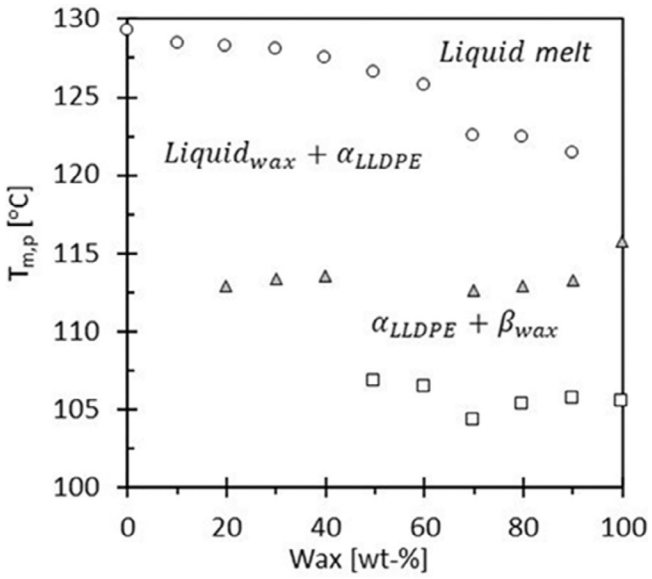

FIGURE 3 Phase diagram based on the loci of the melting peaks associated with the wax-rich β-phases and the linear low-density polyethylene (LLDPE)-rich α-phase driven by composition changes.

the peak temperatures for the wax-rich phases and the LLDPE-rich phase as they evolve with changes in the blend composition. These results reveal significant melting point depression of the LLDPE-rich phase with increasing wax concentration. The melting peaks of the wax-rich phase tends to overlap and ultimately form a relatively high-melting single temperature peak with decreasing wax concentration. Similar miscibility studies in the crystalline phase were previously reported for other wax types.[2,11,19] Chen et al.[11,19] used DSC to investigate the phase morphology of a wide range of paraffin wax-LLDPE blends whereas Gumede et al.[2] studied a 30–70 wax-LLDPE composite. Both groups observed two distinct crystallization endotherms, two distinct crystallization exotherms and significant melting point depression of the polyethylene. The latter is indicative of miscibility in the molten state[2] while the elevation of melting temperature of the wax-rich phase is consistent with co-crystallization with the LLDPE. Therefore, the present results confirm previous results that indicate LLDPE is soluble in molten wax and that it co-crystallizes with the wax.

3.2 | Shear viscosity

Flow curves, for the different compositions of wax-LLDPE, were obtained at temperatures of 160, 170, and 180°C in the rotational shear mode. Figure 4 shows the viscosity (η) versus applied shear rate ($\dot{\gamma}$) results obtained

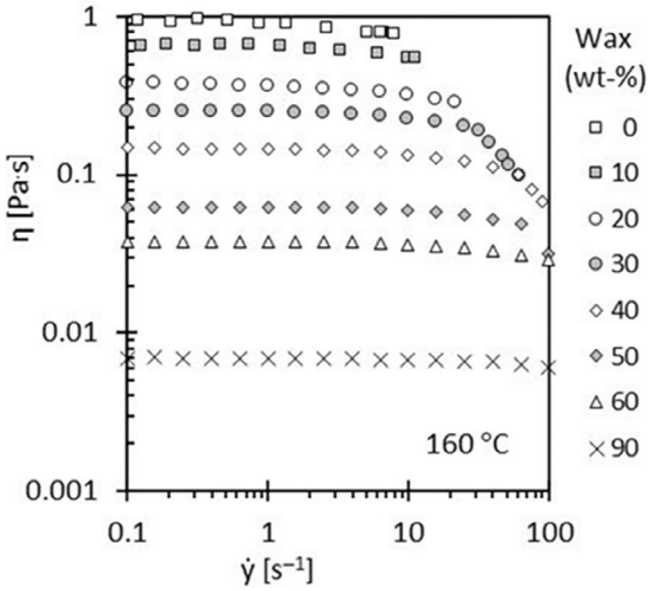

FIGURE 4 Flow curves of the wax-linear low-density polyethylene (LLDPE) melt blends at 160°C.

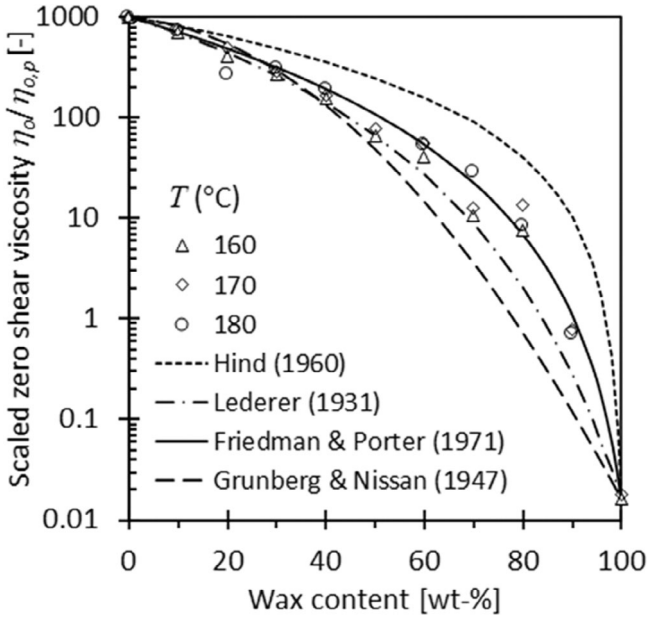

FIGURE 5 Variation of the scaled zero-shear viscosity with wax content. Testing different predictive viscosity mixture rules. The linear and harmonic combining rules were used to fix the η_{12} cross parameter values in the Friedman and Porter and Hind models, respectively.

for selected blends as measured at 160°C. As expected, the apparent viscosity increases in magnitude with increase in LLDPE content. At low shear rates the blends behave like Newtonian fluids. The zero-shear viscosities (η_o) correspond to the plateau values observed at low shear rates, and they are plotted in Figure 5. The flow curves for the LLDPE-rich blends showed shear-thinning behavior at higher shear rates. This apparent decrease in the melt viscosity is caused by progressive disentanglement of the random-coil polymer chains with increase in the applied shear rate. This explains the observations that shear-thinning behavior becomes more pronounced with increase in the LLDPE content. While the wax enhances molecular chain mobility,[12] the viscosity of the blends is dominated by the amount of LLDPE present.

Numerous mixing rules exist which link the variation of Newtonian liquid viscosity to the composition of the fluid. They include the Grunberg and Nissan[20] model

$$\ln\eta = w_p^2 \ln\eta_p + 2w_p w_w \ln\eta_{pw} + w_w^2 \ln\eta_w \quad (1)$$

The Hind et al.[21] model:

$$\eta = w_p^2 \eta_p + 2w_p w_w \eta_{pw} + w_w^2 \eta_w \quad (2)$$

And the Lederer[22] model:

$$\ln\eta = \frac{w_p}{w_p + \beta w_w} \ln\eta_p + \frac{\beta w_w}{w_p + \beta w_w} \ln\eta_w \quad (3)$$

In these equations, w_i represents the mass fraction of component i and the subscripts w and p refer to the wax and polymer respectively.

The adjustable parameter η_{pw} in the Hind et al.[21] and Grunberg and Nissan[20] models represents an interaction viscosity while the constant β in the Lederer model introduces a shift in the composition variable. The utility of these correlative expressions was tested using least squares regression on the zero shear melt viscosity data. The results are shown in Figure 5. The Hind model overestimates the mixture viscosity whereas the other two models underestimate it. Even so, the Lederer model predictions are closest to the actual data.

Sotomayor et al.[12] studied blends of high-density polyethylene with a soft paraffin wax. In effect, they assumed that the Grunberg and Nissan model applies with the following combining rule for the logarithm of the interaction viscosity:

$$\ln\eta_{pw} = \left(\ln\eta_p + \ln\eta_w\right)/2 \quad (4)$$

This assumption reduces the mixing rule to a logarithmic additivity rule:

$$\ln\eta = w_p \ln\eta_p + w_w \ln\eta_w \tag{5}$$

This expression is the expected composition dependence for the "ideal molten liquid mixture." Note that Equation (5) corresponds to a mass fraction-weighted geometric mixing rule for the viscosity:

$$\eta = \eta_p^{w_p}\,\eta_w^{w_p} \tag{6}$$

Equation (5) can be cast in a form that more clearly shows the linear dependence of the logarithm of the blend viscosity on the wax content:

$$\ln\eta = \ln\eta_p + w_w \ln\left(\eta_w/\eta_p\right) \tag{7}$$

In Equation (7), $\ln\eta_p$ is the intercept at $w_w = 0$ and $\ln(\eta_w/\eta_p)$ represents the slope of the straight line on the semi-logarithmic plot of the zero-shear viscosity against mass fraction wax present in the blend. Sotomayor et al.[12] did indeed notice that their data fell more-or-less on a straight line in their plot. However, they only considered samples with a wax content up to 50 wt%. The plots shown in Figure 5 admit a similar linear approximation in this composition range. However, the zero-shear viscosity deviates precipitously from this linear trend at higher wax concentrations. Therefore, Equation (5), or (7), cannot be used to estimate the viscosity of the wax by way of extrapolation to 100 wt% wax in the blend when the only data available contains less than 50 wt% wax.

The F-T wax and the LLDPE share a similar chemical structure. Although the LLDPE also features short branches along the chain, the main difference is in the length of the molecules involved. The melt viscosity of short-chain oligomers increases linearly with molar mass. This applies to the wax and therefore it holds that:

$$\eta_w = K_w M_w \tag{8}$$

where η_w is the Newtonian viscosity of the wax, M_w is the weight-average molar mass of the wax and K_w is a constant that depends on the temperature. Beyond a critical molar mass, the zero-shear melt viscosity increases with the 3.4th power of weight-average molar mass due to the onset of chain entanglement.[23,24] This situation applies to the LLDPE. Therefore:

$$\eta_p = K_p M_p^{\alpha} \tag{9}$$

where η_p is the zero-shear viscosity of the polymer, M_p is the weight-average molar mass of the LLDPE and K_p is a temperature-dependent constant. The exponent takes on a universal value of $\alpha = 3.4$.

The weight average molar mass of a wax-LLDPE blend is given by:

$$M = w_p M_p + w_w M_w \tag{10}$$

where w_w and w_p represent the weight fractions of wax and polymer, respectively, in the binary blend and $w_w + w_p = 1$. If a blend of two low molar mass compounds are considered, combination of Equation (10) with (8) leads to the following mixing rule, which should apply if one mixes two waxes:

$$\eta = w_p \eta_p + w_w \eta_w \tag{11}$$

If, instead a blend of two polymers are considered, combining Equations (10) and (9) leads to the Friedman and Porter[23] mixing rule:

$$\eta = \left(w_p \eta_p^{1/\alpha} + w_w \eta_w^{1/\alpha}\right)^{\alpha} \tag{12}$$

Note that Equation (12) is equivalent to a weighted power-mean mixing rule of order $p = 1/\alpha$.

At the critical molar mass (M_c), Equations (1) and (2) predict the same zero-shear viscosity. This condition links the values of the two viscosity constants:

$$K_w = K_p M_c^{\alpha-1} \tag{13}$$

It is usually assumed that the critical molar mass is a fixed quantity. If that is indeed the case, it implies that the ratio K_w/K_p is temperature independent. In other words, apart from a proportionality constant, the temperature dependence of the constants is the same. Therefore, due to their similar molecular structure, the temperature dependence of the zero-shear viscosity, as applied to wax-polymer blends, is removed if scaling with the viscosity of the neat polymer is done.

Note that the theoretical values for the critical molar mass of polyethylene is $M_c = 2900$ Dalton.[25] The molar mass of the present LLDPE ($M_2 = 129\,100$ Dalton) is much higher than that of the wax ($M_1 = 786$ Dalton). This means that the critical molar mass of the blend was exceeded when as little as 1.6 wt% LLDPE was present in the blend. This is much lower than the lowest LLDPE content (10 wt%) considered presently. Therefore, Equation (12) is likely to provide good data representation for blends forming thermodynamic solutions even though the exponent applicable to the neat wax is unity instead of $\alpha = 3.4$. Figure 6 shows

that this was indeed the case. Surprisingly, the fully predictive Friedman and Porter, Equation (12), provided the much better data fits. It outperformed the conventional viscosity mixture models despite the fact that every single one of the latter models featured an adjustable parameter.

3.3 | Oscillatory rheology

Figure 7A shows representative plots of the complex viscosity (η^*) measured at 160°C for selected wax-LLDPE blends. The complex viscosity was strongly affected by the wax content. The frequency dependence was weak but showed a slight decline on increasing the angular frequency. Measurements made at different temperatures gave similar results. Figure 7B shows the effect of blend composition on the complex viscosity at a fixed angular frequency of 10 rad s^{-1}. Again, a very strong dependence on wax content is observed. The plots against the inverse of the absolute temperature are straight lines indicating an Arrhenius-like temperature dependence[26]:

$$\eta^* = A\exp\left(E_\eta/RT\right) \tag{14}$$

The activation energy was the same for all the composition and equaled 27.5 ± 1.3 kJ mol^{-1}. It was not possible to measure the complex viscosity of the neat wax due to a lack of measurable elastic behavior. Therefore, it was estimated by an extrapolation technique. First it was assumed that the same activation energy applied and that the composition dependence of the complex viscosity also follows the Friedman and Porter mixture rule as defined by Equation (5). The mixture rule exponent and the pre-exponential constant for the wax were fixed by least-squares data regression using the full set shown in Figure 7B. This resulted in $\alpha = 4.81$ and $A = 2.45 \times 10^{-4}$ for the two adjustable parameters. From this, the viscosity of the neat wax was calculated as a function of temperature and plotted as a line in Figure 7B.

An excess complex viscosity can be defined as the difference relative to the complex viscosity of the "ideal molten liquid mixture." The expected value for the latter is defined by Equation (6). From this, the excess complex viscosity can be calculated from the experimentally measured values using:

$$\Delta\eta^* = \eta^* - \eta_1^{w_1}\eta_2^{w_2} \tag{15}$$

where the subscripts 1 and 2 refer to the wax and polymer, respectively.

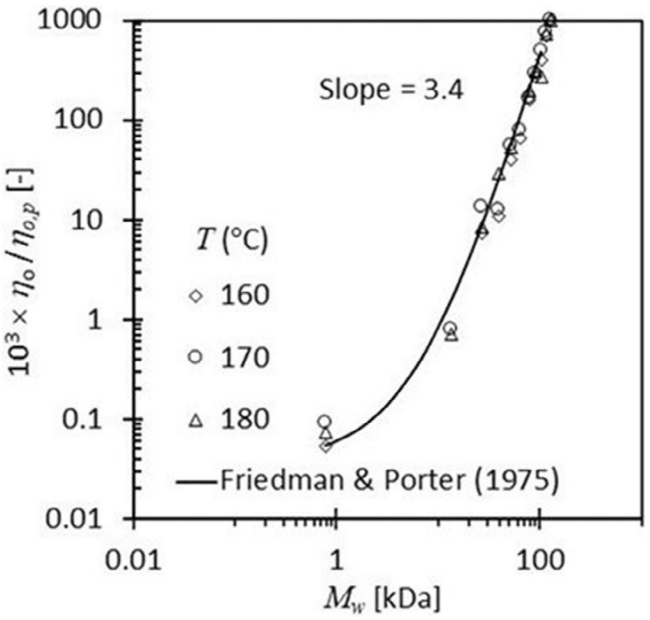

FIGURE 6 Zero-shear viscosity versus the calculated average molecular weight of the blends at various testing temperatures. The Friedman and Porter[23] model is defined by Equation (12) in the text.

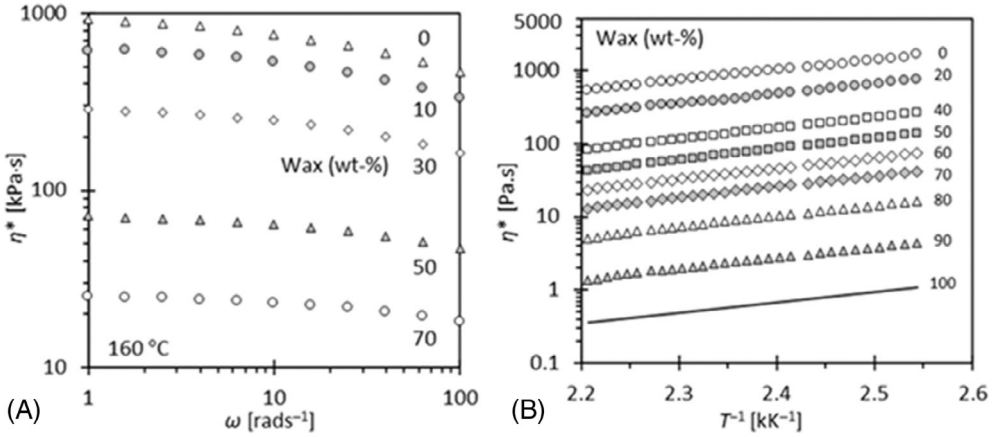

FIGURE 7 (A) Effect of varying the angular frequency and the wax content on the complex viscosity measured at 170°C. (B) Temperature dependence of the complex viscosity measured from 180 to 120°C at a fixed strain of 0.05% and an angular frequency of 10 rad s^{-1}. Note that the values shown for the neat wax represent extrapolated values.

The theoretical expectation, for a system that obeys the Friedman and Porter mixing rule, is given by:

$$\Delta\eta^* = \left[w_1\left(\eta_1^*\right)^{1/\alpha} + w_2\left(\eta_2^*\right)^{1/\alpha}\right]^{\alpha} - \eta_1^{w_1}\eta_2^{w_2} \qquad (16)$$

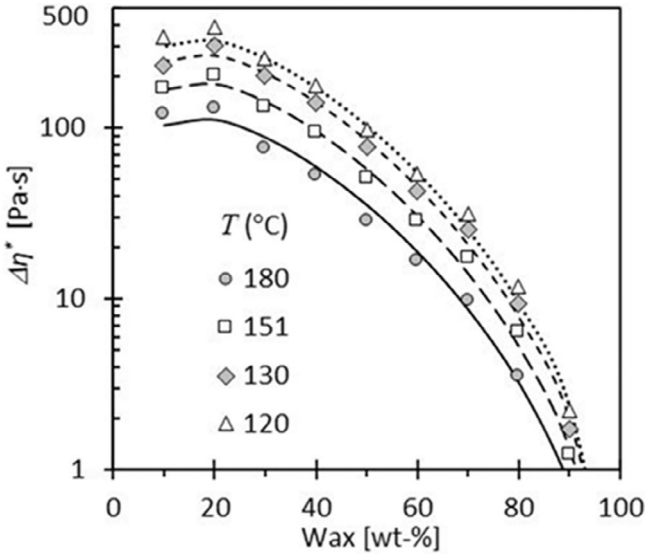

FIGURE 8 Experimental excess complex viscosity data (symbols) calculated using Equation (13) compared to predictions (lines) based on the Friedman and Porter mixture model (with $\alpha = 4.81$) as presented by Equation (15).

Figure 8 compares selected experimental data for $\Delta\eta^*$ with the predictions of Equation (16). Reasonable agreement, between the experimental values and predictions based on the viscosity values of the neat components, is evident. In fact, the SD between experimental and predicted complex viscosity values is 8.1% and the maximum deviation between measured and predicted viscosity was 16%.

The viscoelastic properties of polymer melts are best characterized by the storage and loss moduli. These are linked to the components of the complex viscosity via the following relationships[27]:

$$G'(\omega) = \omega\eta''(\omega) \qquad (17a)$$

and

$$G''(\omega) = \omega\eta'(\omega) \qquad (17b)$$

where ω is the angular frequency; G' and G'' represent the storage modulus (elastic component) and loss modulus (viscous component) of the polymer blend, respectively, and η' and η'' are the real and imaginary components of the complex viscosity.

Figure 9 shows representative log–log plots of the storage and loss moduli as a function of the angular frequency. At the respective measurement temperatures, all

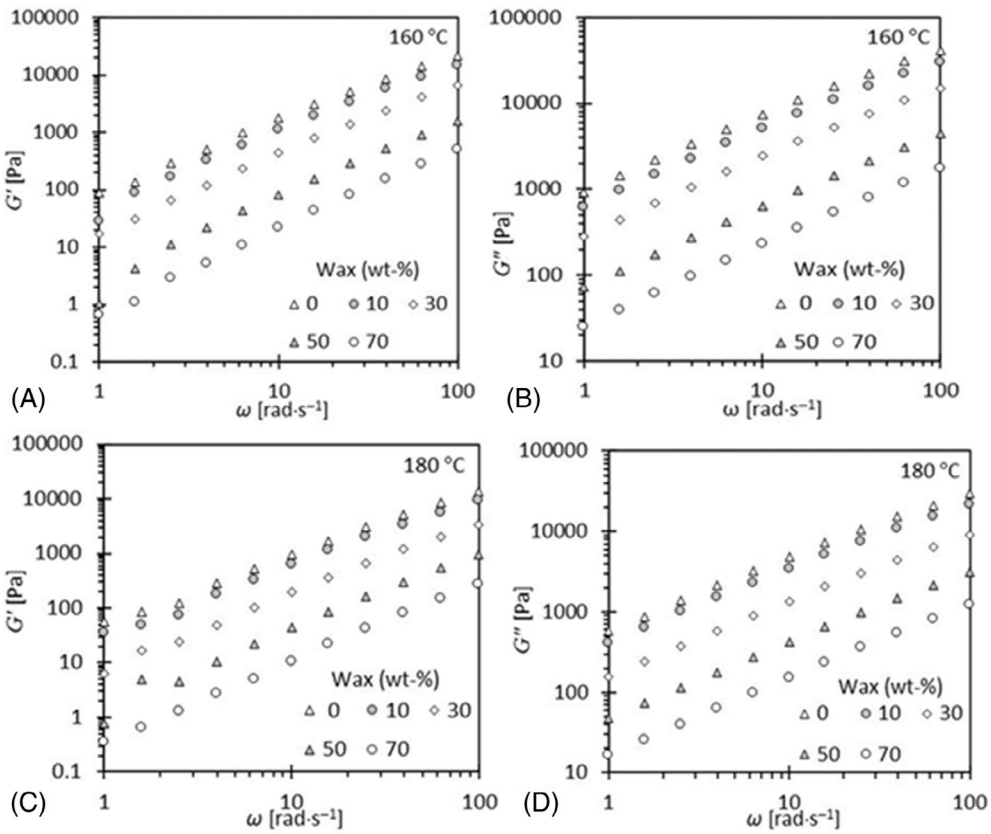

FIGURE 9 Plots of G' and G'' versus ω for selected wax-linear low-density polyethylene (LLDPE) blends measured at 160 and 180°C.

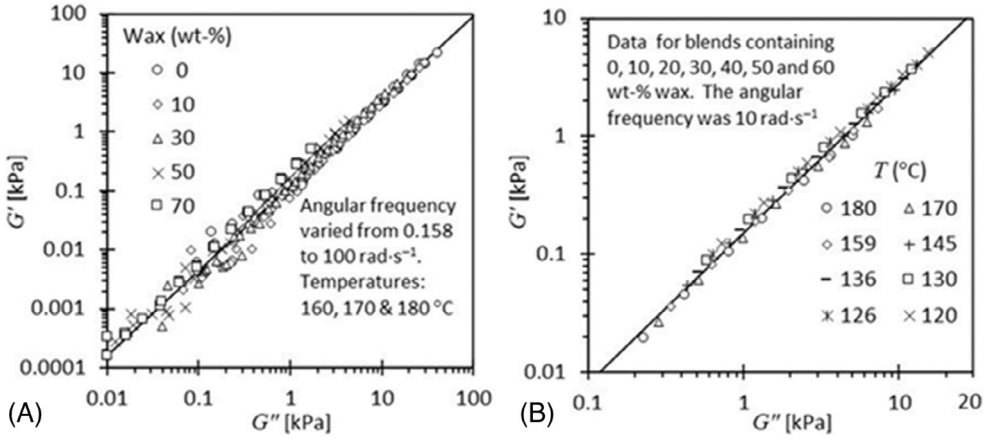

FIGURE 10 Han and Chuang plots of G' versus G'' for wax-linear low-density polyethylene (LLDPE) blends. (A) Emphasizing the effect of blend composition at three different temperatures and five wax content levels. (B) Emphasizing the effect of temperature at seven different wax content levels at a fixed angular frequency of 10 rad s^{-1}.

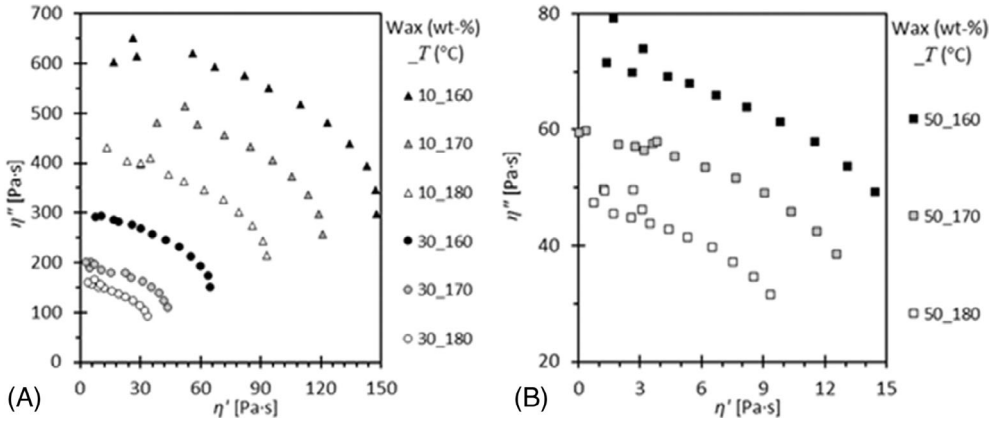

FIGURE 11 Cole–Cole plots of η'' against η' for wax-linear low-density polyethylene (LLDPE) blends.

the blends indicate a more viscous behavior as is indicated by the larger loss modulus. In the case of both moduli, a logarithmic-linear dependence on the angular frequency is indicated. The slope of the lines of loss modulus are lower than those of the storage modulus. The slope of the logarithm of the storage modulus with respect to the logarithm of the angular frequency is approximately equal to 5/4. It increases with wax content reaching a value of ~3/2 at a wax content of 70 wt%. The corresponding slopes of the logarithm of the loss modulus with respect to the logarithm of the angular frequency is less affected by composition. It is about 0.85 for the neat LLDPE and increases to about 0.94 for the blend with 70 wt% wax.

Rheological investigation of oscillatory shear flow behavior, obtained on melts, can provide information on the nature of the liquid phase.[28,29] A Han plot of log G' versus log G'' can be used to detect liquid–liquid phase separation in thermoplastic polymer blends. In general, linear temperature-independent and composition-independent Han plots are indicative of homogenous single-phase behavior of liquid melts.[28] Figure 10 shows such plots for the current wax-LLDPE blends. The indicated data trends confirm the thermodynamic compatibility of the present wax-LLDPE blends in the molten liquid state at temperatures as low as 120°C.

Cole–Cole plots also provide information on the miscibility of blends in the molten state.[30–33] Semi-circular shapes of plots of the imaginary viscosity (η'') against the real viscosity (η') imply miscibility. Figure 11A,B shows that this was indeed the case for the for all the blends analyzed for present wax-LLDPE system. This provides additional evidence for the miscibility of wax and LLDPE in the fully molten state.[32,33]

4 | CONCLUSION

Polyolefins used as base polymer matrix for large volume plastic applications are often rigid and stiff. This property makes it difficult to process using conventional processing techniques. To ensure the necessary flexibility and adequate flow properties during processing, additives such as polyethylene wax are often added. This study explored F-T wax-based processing agents in combination with low molecular weight LLDPE as a low-cost alternative.

The phase behavior of blends of an experimental F-T wax and a LLDPE was explored. DSC results showed LLDPE melting point depression indicating solubility of the polymer in the molten wax. Furthermore, the DSC traces for the blends differed substantially from linear combinations of the parent materials. This supports partial crystallization of the polymer with the wax and also of the wax with the polymer.

Rheological information on F-T wax polyethylene blends over the total composition range is lacking, the following results are obtained to fill that gap. The composition dependence of the zero-shear viscosity agreed with the predictions of the Friedman and Porter model for molten mixtures controlled by polymer chain entanglements. The composition dependence of the complex viscosity followed a similar mixture rule except that the exponent differed from the one applicable to the zero-shear viscosity, that is, $\alpha = 4.81$ instead of $\alpha = 3.4$. The complex viscosity of all the blends obeyed an Arrhenius-like temperature dependence with an activation energy of 27.5 ± 1.3 kJ mol^{-1}. Plots of log G' versus G'' (so-called Han plots) were linear and essentially independent of composition, temperature and the applied angular frequency. The Cole–Cole plots also indicated that the wax-LDPE blends are miscible at melt state. Together, these confirmed the miscibility of the wax and the LLDPE down to temperatures as low as 120°C.

AUTHOR CONTRIBUTIONS

Thobile Mhlabeni: Conceptualization; data curation; formal analysis; investigation; methodology; writing – original draft. **Cebo Ngobese:** data curation; formal analysis; investigation. **Shatish Ramjee:** formal analysis; methodology; conceptualization; validation, supervision; project administration; writing – review and editing. **Walter Focke:** formal analysis; methodology; conceptualization; validation; funding acquisition; project administration; supervision; writing – review and editing.

ACKNOWLEDGMENTS

Generous financial support from Sasol is gratefully acknowledged.

DATA AVAILABILITY STATEMENT

The data that support the findings of this study are available from the corresponding author, Shatish Ramjee, upon request.

ORCID

Thobile Mhlabeni https://orcid.org/0000-0002-5698-0533

Shatish Ramjee https://orcid.org/0000-0003-0104-207X

Walter Focke https://orcid.org/0000-0002-8512-8948

REFERENCES

[1] J. A. Molefi, A. S. Luyt, I. Krupa, *Thermochim. Acta* **2010**, *500*, 88.
[2] T. P. Gumede, A. S. Luyt, R. A. Pérez-Camargo, A. Iturrospe, A. Arbe, M. Zubitur, A. Mugica, A. J. Mülleral, *J. Polym. Sci. Part B: Polym. Phys.* **2016**, *54*, 1469.
[3] T. P. Gumede, *J. Vinyl Addit. Technol.* **2021**, *27*, 469.
[4] R. K. Tewo, H. Rutto, W. Focke, T. Seodigeng, L. Koech, *Rev. Chem. Eng.* **2019**, *35*, 335.
[5] L. Novakova-Marcincinova, J. Novak-Marcincin, *Adv. Mater. Res.* **2013**, *740*, 597.
[6] M. Khalil, H. Radwan, F. Annuar, H. Azmi, M. Z. Zakaria, *J. Adv. Res. Des.* **2015**, *6*, 11.
[7] M. Gale, *Adv. Polym. Technol.* **1997**, *16*, 251.
[8] A. S. Luyt, R. Brüll, *Polym. Bull.* **2004**, *52*, 177.
[9] H. S. Mpanza, A. S. Luyt, *Polym. Test.* **2006**, *25*, 436.
[10] M. J. Hato, A. S. Luyt, *J. Appl. Polym. Sci.* **2007**, *104*, 2225.
[11] F. Chen, M. P. Wolcott, *Euro. Polym. J.* **2014**, *52*, 44.
[12] M. E. Sotomayor, I. krupa, A. Várez, B. Levenfeld, *Renew. Energy* **2014**, *68*, 140.
[13] R. Esmaeilzade, F. Sharif, R. Rashedi, A. Dordi Nejad, *J. Appl. Polym. Sci.* **2022**, *139*, 51750.
[14] A. Y. Coran, C. E. Anagnostopoulos, *J. Polym. Sci.* **1962**, *57*, 13.
[15] A. Nakajima, F. Hamada, *Kolloid Z. Z. Polym.* **1965**, *205*, 55.
[16] J. Martínez-Salazar, A. Alizadeh, J. J. Jiménez, J. Plans, *Polymer* **1996**, *37*, 2367.
[17] L. Radebe, J. Wesley-Smith, W. W. Focke, S. Ramjee, *J. Polym. Eng.* **2023**, *43*, 80.
[18] L. Radebe, J. Wesley-Smith, W. W. Focke, S. Ramjee, *J. Polym. Eng.* **2023**, *43*, 13.
[19] F. Chen, M. Wolcott, *Sol. Energy Mater. Sol. Cells* **2015**, *137*, 79.
[20] L. Grunberg, A. H. Nissan, *Nature* **1949**, *164*, 799.
[21] R. K. Hind, E. McLaughlin, A. R. Ubbelohde, *Trans. Faraday Soc.* **1960**, *56*, 328.
[22] E. Lederer, *Kolloidchem. Beih.* **1931**, *34*, 270.
[23] E. M. Friedman, R. S. Porter, *Trans. Soc. Rheol.* **1975**, *19*, 493.
[24] L. Fetters, D. Lohse, R. Colby, in *Physical Properties of Polymers Handbook* (Ed: J. E. Mark), Springer, New York, NY **2007**.
[25] F. J. Stadler, C. Piel, J. Kaschta, S. Rulhoff, W. Kaminsky, H. Münstedt, *Rheol. Acta* **2006**, *45*, 755.
[26] H. Eyring, J. Hirschfelder, *J. Phys. Chem.* **1937**, *41*, 249.
[27] J. D. Ferry, *J. Am. Chem. Soc.* **1961**, *83*, 4110.
[28] C. D. Han, H. K. Chuang, *J. Appl. Polym. Sci.* **1985**, *30*, 4431.
[29] C. D. Han, M. S. Jhon, *J. Appl. Polym. Sci.* **1986**, *32*, 3809.
[30] P. Agrawal, M. H. A. Silva, S. N. Cavalcanti, D. M. G. Freitas, J. P. Araújo, A. D. B. Oliveira, T. J. A. MéloP, *Polym. Bull.* **2022**, *79*, 2321.
[31] L. Bai, Y. M. Li, W. Yang, M.-B. Yang, *J. Appl. Polym. Sci.* **2010**, *118*, 1356.
[32] K. Cho, B. H. Lee, K.-M. Hwang, H. Lee, S. Choe, *Polym. Eng. Sci.* **1998**, *38*, 1969.
[33] L. A. Utracki, *Two Phase Polymer Systems*, Hanser Publishers, Munich **1991**.

AUTHOR BIOGRAPHIES

Thobile Mhlabeni is currently a PhD student in the Department of Chemical Engineering and the Institute of Applied Materials, University of Pretoria, South Africa. She is a published author in the field of polymer materials and nanoscience. Her interests include research on mixture models to characterize physico-chemical properties of polymer mixtures and enhanced oil recovery technologies.

Cebo Ngobese is a graduate of the University of Pretoria, having completed his Bachelor of Engineering in Chemical Engineering and is pursuing an honours degree in Technology Management at the University of Pretoria. He has collaborated with the Institute of Applied Materials on polymer processing projects focused on polymer additives. He is interested in polymer processing, material characterisation, and thermodynamics.

Shatish Ramjee is a senior lecturer in the Department of Chemical Engineering, University of Pretoria. He obtained his masters and PhD in chemical engineering from the Universtiy of Pretoria. His research interests are in applied rheology and modelling. This is primarily in the fields of carbon and polymer materials science, emulsions, and minerals processing.

Walter Focke is a professor emeritus of the Department of Chemical Engineering, University of Pretoria. He holds a master's degree in Chemical Engineering from the University of Pretoria and a PhD from MIT in Materials Science and Engineering. His research interests are in polymer additive technology and polymer-based controlled release systems for insect pest control.

How to cite this article: T. Mhlabeni, C. Ngobese, S. Ramjee, W. Focke, *J. Vinyl Addit. Technol.* **2023**, *29*(4), 698. https://doi.org/10.1002/vnl.21984